ILASS–Europe 2019, 29th Conference on Liquid Atomization and Spray Systems, 2-4 September 2019, Paris, France

A modified Young-Laplace approach to dynamic wetting of dilute polymer solutions

Volfango Bertola*
University of Liverpool, School of Engineering, Laboratory of Technical Physics, Liverpool L69 3GH, United Kingdom
*Corresponding author: Volfango.Bertola@liverpool.ac.uk

Abstract
The impact of viscoelastic dilute polymer solution drops on hydrophobic surfaces is re-visited in the context of dynamic wetting. Dilute polymer solutions are widely used, for example, in the formulation of agrochemicals, printing and additive manufacturing inks, and their drops have a tendency to stick to hydrophobic surfaces as opposed to Newtonian drops of similar viscosity, which tend to bounce off. However, the physical mechanism responsible for the peculiar impact behaviour of dilute polymer solution drops is poorly understood to date. This work attempts to interpret the impact behaviour of dilute polymer solution drops in terms of wetting, using a modified Young-Laplace approach in the neighbourhood of the unstable equilibrium corresponding to maximum spreading.

Keywords
Dynamic wetting; Dilute polymer solutions; Drop impact; Coil-stretch transition.

Introduction

The wetting dynamics of dilute polymer solutions can be remarkably different from the case of simple Newtonian liquids, revealing significant differences in the behaviour of the moving contact line during the spreading and/or receding phase, in the amplitude of the dynamic contact angle, as well as in the intrinsic time of the phenomenon. A well-known example is the so-called anti-rebound effect of polymer additives. When a droplet of water falls on to a hydrophobic surface, such as the waxy leaf of a plant, the drop is often observed to bounce off. However, for almost 20 years it has been known that the addition of very small quantities ($\approx$100 ppm) of a flexible polymer such as polyethylene oxide (PEO) can completely prevent rebound, by reducing the recoil velocity of the drop after the inertial spreading of two orders of magnitude [1, 2]. This is surprising since the shear viscosity and surface tension of such drops are almost identical to those of pure water.

Initially, the phenomenon was attributed either to the elongational viscosity [1, 2] or to normal stresses [3] arising in dilute polymer solutions, and wetting was explicitly excluded from the potential causes. However, these early approaches revealed a number of weaknesses [4], which suggested to reconsider an interpretation of the phenomenon in terms of dynamic wetting, as initially suggested by Rozhkov et al. [5]. Particle velocimetry measurements inside impacting drops [6, 7] demonstrated that velocities and velocity gradients are similar for Newtonian and non-Newtonian drops, excluding a potential role of elongational viscosity. High-speed measurements of the apparent dynamic contact angle of impacting drops [8, 9] showed that in dilute polymer solution drops the receding contact angle is significantly smaller than in drops of pure solvent, in contrast to initial claims [1]. In addition, if the dilute polymer solution is doped with fluorescent λ-DNA molecules, stretched DNA molecules can be observed on the substrate behind the receding contact line [6], oriented in the direction perpendicular to the contact line. This suggests the force balance at the contact line might include a polymer stretching component, which from a macroscopic point of view can be interpreted as an additional, dissipative force acting on the contact line and opposed to its movement, or an effective contact line friction. by forced dewetting experiments of dilute polymer solution drops, where the contact line velocity was controlled by removing the fluid with a syringe pump [10].

More recently, high-speed, high-magnification images revealed that, as opposed to pure water, the contact line of dilute polymer solutions is pinned at several points on the impacting surface, and the polymer solution forms dendritic structures and filaments on the substrate [11, 12], slowing down the recoiling phase and leading to the formation of secondary droplets having diameter size comparable to the filaments width (15 μm). The ensemble of polymer molecules stretching as the drop edge sweeps the surface provide the dissipative force necessary to slow down the displacement of the contact line. This can be interpreted, from a macroscopic point of view, as an additional, dissipative force acting on the contact line and opposed to its movement, or an effective contact line friction. This also explains the reduction of the dynamic contact angle observed in experiments: to overcome the action of polymer molecules on the contact line, the horizontal component of the surface force driving the droplet retraction must be larger than in a Newtonian fluid, therefore the apparent dynamic contact angle must be smaller. In the present work, the Young-Laplace force balance is modified by introducing an additional term representing the polymer stretching force, obtained explicitly using the classical finite extensibility approach. The proposed mechanism explains both qualitatively and quantitatively, in terms of orders of magnitude, the strong reduction of the apparent contact angle and of the receding contact line velocity observed in dilute polymer solution drops as compared with drops of pure solvent.

Experimental observations

The impact morphology of dilute polymer solution drops impacting on hydrophobic sutfaces has been extensively investigated experimentally, both from a qualitative and from a quantitative point of view. The main findings can be summarised as follows:

- The contact line receding velocity of dilute polymer solution drops is at least two orders of magnitude smaller than the receding velocity of drops of pure solvent [1, 2, 13];
- The bulk velocity of the fluid, as well as the velocity gradients, are similar in drops of pure solvent and drops of dilute polymer solutions [5, 6, 7, 14];
- The receding contact angle of dilute polymer solution drops is significantly smaller than that of drops of pure solvent, while the advancing contact angle is identical [8, 9];
- Polymer molecules deposited on the substrate can be observed after the transit of the receding contact line [6, 14, 10];
- The receding contact line of polymer solution drops stretches microscopic liquid filaments in the radial direction, which cannot be observed in drops of pure solvent [4, 11, 12].

The main parameters that influence the drop impact behaviour are the impact Weber number, $We = \rho U^2 D_0/\gamma$, where ρ is the fluid density, γ the surface tension, U the impact velocity,and D_0 the equilibrium drop diameter, and the polymer concentration; since most studies involve fluids of comparable shear viscosity, usually the other dimensionless parameters relevant to drop impact, the Reynolds and the Ohnesorge numbers, are not cosidered.

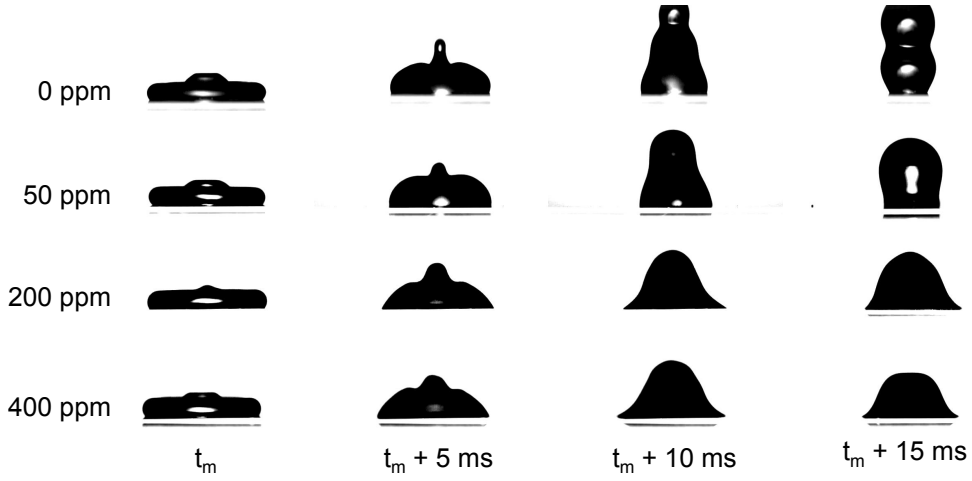

Figure 1. Side views of impacting drops, for impact Weber number We = 15; the initial time , t_m, corresponds to maximum spreading.

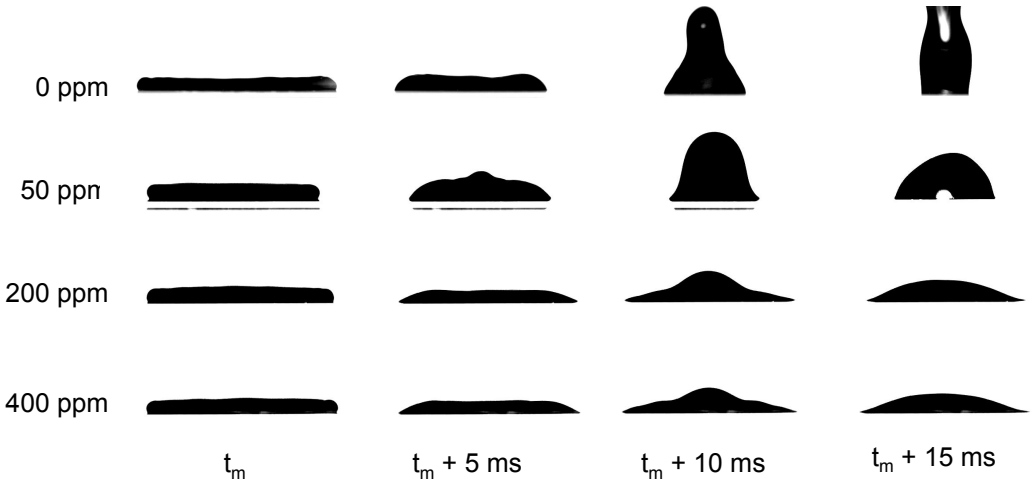

Figure 2. Side views of impacting drops, for impact Weber number We = 80; the initial time , t_m, corresponds to maximum spreading.

The maximum concentration of dilute polymer solutions is limited by the overlap concentration, which is often calculated using the Mark-Houwink relationship, $c_o = aM^b$ [17], where M is the molecular weight, and is of the order of 500 ppm for the most common long-chain polymers. In this regime viscosity and the relaxation time, τ, are approximately a linear and a square root function of the polymer concentration, respectively [18], while the surface tension is approximately the same as the solvent on the timescale of experiments [19].
The typical morphology of dilute polyethylene oxide (PEO) aqueous solution drops with different polymer concentrations impacting on a PTFE surface during the retraction stage is displayed in Figures 1 and 2, respectively for impact Weber numbers $We = 15$ and $We = 80$.
At maximum spreading, the contact angle is approximately the same for all polymer concentrations, irrespective of the impact Weber number, and is equal, within the measurement error, to the advancing contact angle of water on PTFE. During the drop retraction, the contact angle of polymer solution drops becomes significantly smaller than the contact angle of water drops; however, one can observe that the receding contact angle magnitude strongly depends on the liquid flow during drop recoil, which moves radially from the liquid rim to the centre of the lamella and vice-versa, and determines the shape of the drop free surface. Thus, the apparent contact angle does not result exclusively from the dynamic force balance at the contact line.
Figures 3 and 4 display, respectively, the dimensionless base diameter and the apparent contact angle during the first 50 ms after impact, for impact Weber numbers We = 15 and We = 80. In both cases, the inertia-dominated spreading is almost identical for all solutions, however there is a clear difference between the retraction dynamics of water drops and that of any polymer solution; whilst water drops exhibit a fast recoil, eventually leading to full or partial rebound after about 40 ms, where $D/D_0 \to 0$, and limited dynamic hysteresis between the advancing and receding contact angles polymer solution drops have a slow retraction dynamics, characterised by ample oscillations of the apparent contact angle (see Figure 4a).

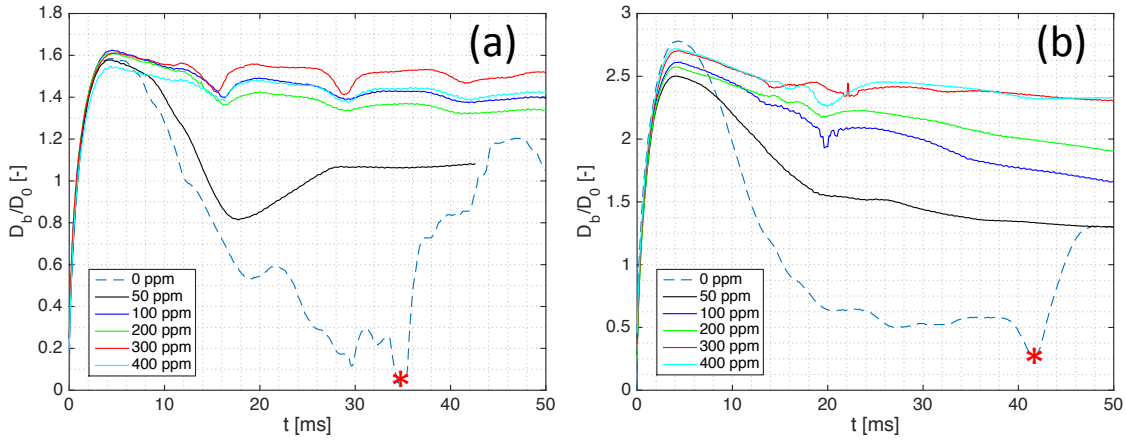

Figure 3. Dimensionless base diameter of impacting droplets with different polymer concentrations, for impact Weber numbers We = 15 (a) and We = 80 (b); the asterisk marks the instant of drop rebound.

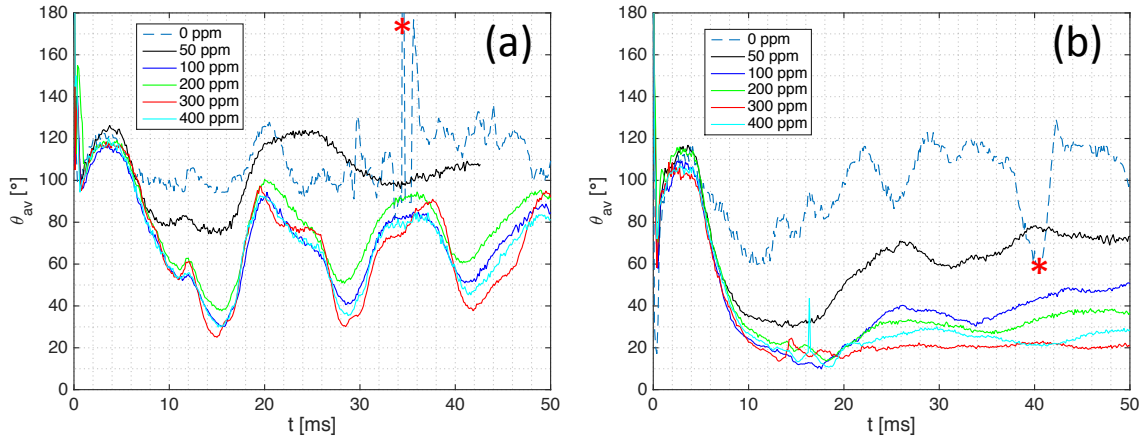

Figure 4. Average apparent contact angle of impacting droplets with different polymer concentrations, for impact Weber numbers We = 15 (a) and We = 80 (b); the asterisk marks the instant of drop rebound.

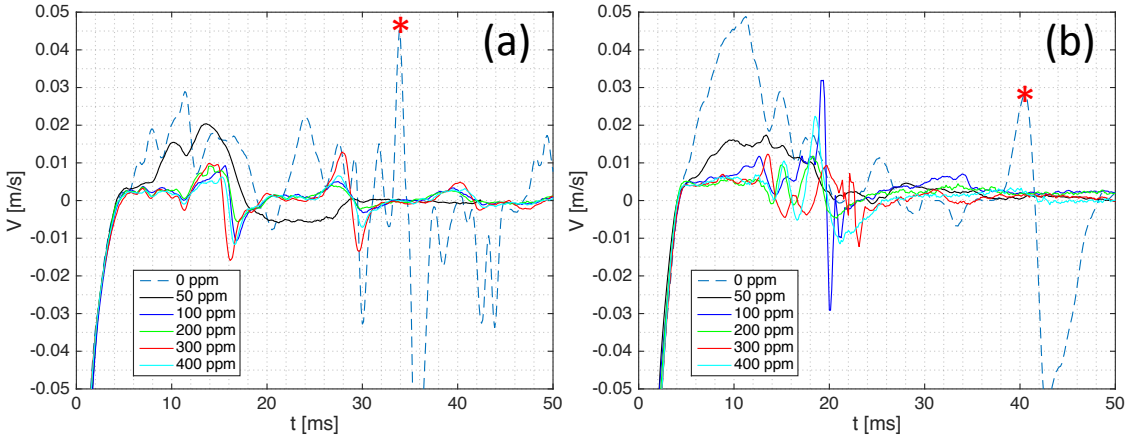

Figure 5. Contact line velocity (positive in the direction of recoil) of impacting droplets with different polymer concentrations, for impact Weber numbers We = 15 (a) and We = 80 (b); the asterisk marks the instant of drop rebound.

These oscillations are associated with a peculiar stick-slip behaviour of the contact line, which has a sharp acceleration in the direction of retraction followed by a quick expansion, generating a series of local minima in the base diameter time series (see Figure 3a); the local minima of the base diameter, i.e., the points where the contact line velocity changes its sign, correspond to the local minima of the apparent contact angle. Such behaviour becomes weaker at higher Weber numbers, where the base diameter decreases monotonically with only one stick-slip event corresponding to the absolute minimum of the apparent contact angle, as shown in Figures 3b and 4b.
In all cases, the behaviour of polymer solution drops with polymer concentrations of 100 ppm and above is almost identical, especially in the first stages of recoil, while polymer solution drops with a polymer concentration of 50 ppm exhibit an intermediate behaviour between drops of pure water and drops of the other polymer solutions.
The contact line velocity, calculated from the base diameter data of Figure 3, is displayed in Figure 5. During the initial 4-5 ms after impact, the velocity magnitude decreases steeply until the drops reaches the maximum spreading; during this inertial spreading stage, the advancing contact line velocity of polymer solution drops is identical to that of water drops, and independent of the polymer concentration. As the recoil stage begins, the contact line velocities of water drops and polymer solution drops diverge; the receding contact line velocity of water drops is significantly larger than that of polymer solution drops and exhibits large oscillations during which it may change sign (i.e., the contact line may advance for short periods of time during drop recoil). In polymer solution drops, the receding contact line velocity remains practically constant at the beginning of recoil, and then exhibits oscillations of smaller amplitude than that of water drops, which are quickly dampened as recoil proceeds.
The comparison of Figures 4 and 5 also indicates that the contact line recoil starts when the contact angle is still larger than 90°. This inertial effect appears as a hysteresis loop dependent on the Weber number in the contact angle vs. contact line velocity plot, and proves that the contact line dynamics of impacting droplets is not driven solely by wetting.

Discussion

The hydrodynamics of the liquid wedge near the contact line during drop retraction can be modelled as the flow between a fixed horizontal surface (the substrate) and a plate inclined at an angle θ (corresponding to the instantaneous value of the apparent dynamic contact angle), moving at velocity U, as shown schematically in Figure 6a. The minimum thickness of the liquid film, h_0, must be no less than the unperturbed size of the polymer coils, R_0; for polyethylene oxide molecules in water, one finds $R_0 = 0.0888M^{1/2} = 178$ nm, where M is the molecular weight [16, 17], hence one can take an order of magnitude $h_0 \approx 0.2\mu$m. Polymer coils are subject to hydrodynamic interaction with the solvent, with a characteristic Zimm time $\tau_Z \approx 0.2\eta_s R_0^3/k_BT = 0.27$ ms and a Rouse time $\tau_R \approx 2R_h\eta_s R_0^2/\pi k_BT = 0.41$ ms, where η_s is the solvent viscosity.
At this point, it is important to note that the magnitude of U, i.e. the main parameter of the process, is not necessarily equal to the contact line velocity during drop retraction. Previous works [4, 6, 7] show that while in water drops the fluid velocity is the same as the velocity of the receding contact line, in dilute polymer solution drops the contact line velocity is two or three orders of magnitude smaller than the bulk velocity of the fluid during retraction.
In a reference frame originating on the contact point, the velocity components parallel and perpendicular to the substrate during drop retraction are, respectively, $u \approx Uy/h(x)$ and $v \approx \xi(\theta)x$, where $h(x) \approx \theta x$ is the liquid film thickness and $\xi(\theta)$ is a positive function of the apparent contact angle (see Figure 6a). Since the order of magnitude of the receding contact line velocity is $U \approx 10^{-2} - 10^{-3}$ m/s [1, 2, 6, 7, 9], $U\tau_Z/h_0 \gg 1$.
The velocity gradient of this flow field can be split into its symmetrical part, $A = \frac{1}{2}(u_y + v_x) = \frac{1}{2}(U/h + \xi)$, associated with a pure deformation, and its anti-symmetrical part $\omega = \frac{1}{2}(u_y - v_x) = \frac{1}{2}(U/h - \xi)$, associated with a pure rotation. Since $\xi(\theta) > 0$, $\omega/A < 1$ therefore it is possible to have strong distortions of the polymer coils, even in the absence

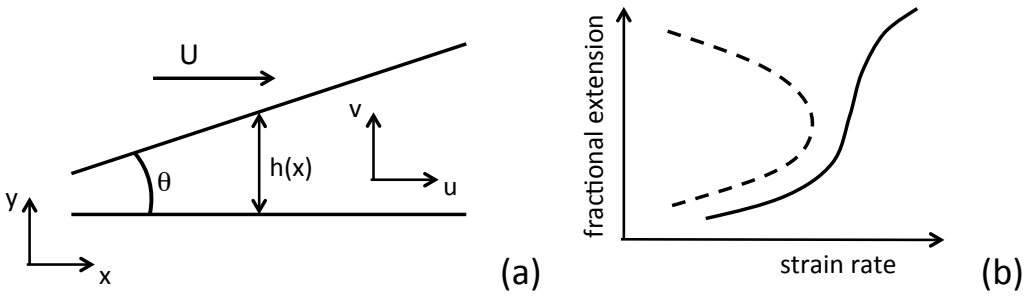

Figure 6. Schematic of the liquid wedge near the contact line (a) and schematic of supercritical coil-stretch transition [21] (b).

of elongational flow [20]. This corresponds to a second–order transition from coil to stretch conformation state, i.e. with a constantly positive slope of the stretching ratio, $l = r/L$, where r is the polymer elongation and L the length of the fully stretched chain, with respect to the order parameter $\xi(\theta)$ (i.e., $dl/d\xi > 0$), as illustrated schematically in Figure 6b [21].
Following the classical finite extensibility approach [22], the stretching ratio is related to the velocity gradient as:

$$l = \frac{3}{Z\mathcal{L}^{-1}(l)} \left\{ 1 + \frac{1}{6} \frac{\left(\frac{U}{h} + \xi\right)^2 \tau^2}{\frac{9l^2}{\left[\mathcal{L}^{-1}(l)\right]^2} - \frac{U}{h}\xi\tau^2} \right\} \tag{1}$$

where τ is the relaxation time, which is given by [21]:

$$\tau(l) \approx \frac{\tau_R}{1 + \frac{1}{l}} \tag{2}$$

and $\mathcal{L}^{-1}(l)$ is the inverse Langevin function, which can be estimated, for example, using Kroger's approximation [23]:

$$\mathcal{L}^{-1}(l) = \frac{3l - (l/5)(6l^2 + l^4 - 2l^6)}{1 - l^2} \tag{3}$$

The resulting recall force of a stretched polymer coil is:

$$F = \frac{k_B T L}{R_0^2} \mathcal{L}^{-1}(l) \tag{4}$$

Figures 7a and 7b display, respectively, the polymer molecule elongation, $l = r/L$, and the recall force of a single polymer molecule as a function of the receding velocity, U, calculated from the numerical solution of Eqs. (1-4). These figures show that in a shear layer corresponding to the cut-off thickness of the polymer solutions contact line ($h \approx 0.2\mu$m), one obtains appreciable stretching of polymer molecules for velocities $U \gtrsim 350$ mm/s. Thus, the receding contact line velocity (Figures 5a and 5b) is not sufficient to achieve a significant stretching.
Particle velocimetry measurements inside a recoiling droplet of a 200 ppm polyethylene oxide solution, in a horizontal plane approximately 10 μm above the impact surface, indicate fluid velocities between 200 and 300 mm/s [6, 7], which means the hydrodynamic conditions to induce a significant stretching of polymer molecules do not occur during drop recoil after maximum spreading.

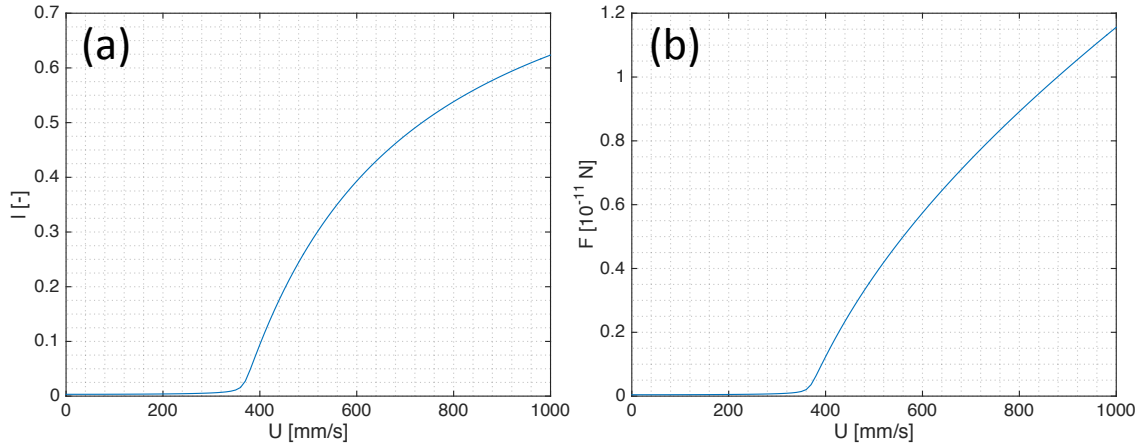

Figure 7. Polymer elongation, $l = r/L$ (a), and recall force of a stretched molecule (b) as a function of the fluid velocity, U.

Thus, one must conclude the supercritical coil-stretch transition occurs during the inertial spreading of the droplet, because of the large shear rates (of the order of 10^3 s^{-1}) arising in the expanding lamella. This also explains why at the very beginning of drop recoil there is no transient buildup of a polymer force on the contact line characterised by a large retraction velocity; if polymer molecules are already stretched at maximum spreading, the magnitude of the polymer force is maximum at the beginning of recoil.
Based on the ensemble of experimental evidence, one can formulate a hypothesis about the behaviour of polymer solution drops impacting onto solid surfaces:

- The large shear velocity gradients in the lamella during the inertial spreading stage cause a spercritical coil-stretch transition of polymer molecules; in these conditions, it was found polymers reach a mean fractional extension $l \approx 0.5$, characterised by a practically flat probability density between $l \approx 0.1$ and $l \approx 0.7$ [24]; this is consistent with the direct observation of stretched DNA molecules [6] and of thin liquid filaments breaking down with the well-known beads-on-a-string mechanism [11, 12] behind the receding contact line.

- At the beginning of drop recoil, i.e. when the contact line velocity changes sign, which occurs when the contact angle is still $> 90^\circ$, the partially stretched polymer molecules on the de-wetted substrate induce a recall force on the receding contact line, opposed to the contact line velocity, which acts to further stretch polymer molecules in a similar fashion to molecular combing [25]; this can be interpreted, from a macroscopic point of view, as an additional, dissipative force acting on the contact line and opposed to its movement, or an effective contact line friction.

- The polymer force eventually decays exponentially in time, depending on the relaxation time of the polymer solution.

The above process translates into the following expression for an overall average polymer force per unit length acting on the contact line and opposed to its velocity:

$$F_P = \sqrt{n}\frac{k_B T L}{R_0^2}\mathcal{L}^{-1}(0.5)\left[\exp\left(\frac{t-t_0}{\tau_S}\right)\right]\frac{-v_R}{|v_R|} \tag{5}$$

where $n = \rho_P c' N_A/M$ is the bulk number density of polymer coils in the fluid wedge (rho_p is the polymer density, N_A Avogadro's number, c' the volume concentration of the polymer, and M its molecular mass). The polymer coils that are stretched as the contact line sweeps the substrate align in a thin layer at the bottom of the fluid wedge, therefore their number scales as $\approx \sqrt{n}$. According to Eq. (3), the value of the inverse Langevin function corresponding to 50% fractional stretching is $\mathcal{L}^{-1}(0.5) = 1.7958$. Finally, v_R is the receding contact line velocity, t_0 the time corresponding to the start of recoil, and τ_S the relaxation time of the polymer solution, which in the case of polyethilene oxide can be calculated using the following correlation [18]:

$$\tau_S = \sqrt{c}\left(1.82\cdot 10^{-3}[\eta]_0 - 2.9\cdot 10^{-11}[\eta]_0^3 - 0.51\right)\exp\left(-0.0004T^2\right) \tag{6}$$

where $[\eta]_0 = 0.0125M^{0.78}$ is the characteristic viscosity [17], c is the polymer mass concentration, and T the solution temperature in $^\circ$C.
The polymer force given by Eq. (5) is parallel to the impact surface, therefore it combines with the component of the Young-Laplace force per unit length in the same direction [26]:

$$F_{YL} = \gamma\cos\theta_P \tag{7}$$

where γ is the surface tension, and θ_P the apparent contact angle of polymer solution drops.
The dimensionless Young-Laplace and polymer forces per unit length, F_{YL}/γ and F_P/γ, are plotted in Figure 8, for different polymer concentrations and different Weber numbers. Firstly, one can observe the two forces have the same order of magnitude, which suggests Eq. (5), obtained without any empirical adjustments to experimental data, provides a realistic description of the phenomeon. Secondly, when the two forces are opposed the apparent contact angle decreases, i.e. the Young-Laplace force grows, while when they have the same sign the contact angle increases, therefore reducing the Young-Laplace contribution to the dynamic force balance, which in a system out of equilibrium with receding contact line can be written as:

$$\gamma\cos\theta_P > F_P \tag{8}$$

This effect can be clearly observed at low Weber numbers (Figures 8a-8c), while at higher Weber numbers (Figures 8d-8f) the influence of the liquid inertia on the Young-Laplace force is predominant. Thus, although the proposed mechanism explains both qualitatively and quantitatively (in terms of orders of magnitude) the strong reduction of the apparent contact angle and of the receding contact line velocity observed in dilute polymer solution drops as compared with drops of pure solvent, it cannot predict their values accurately because it does not account for inertial effects.

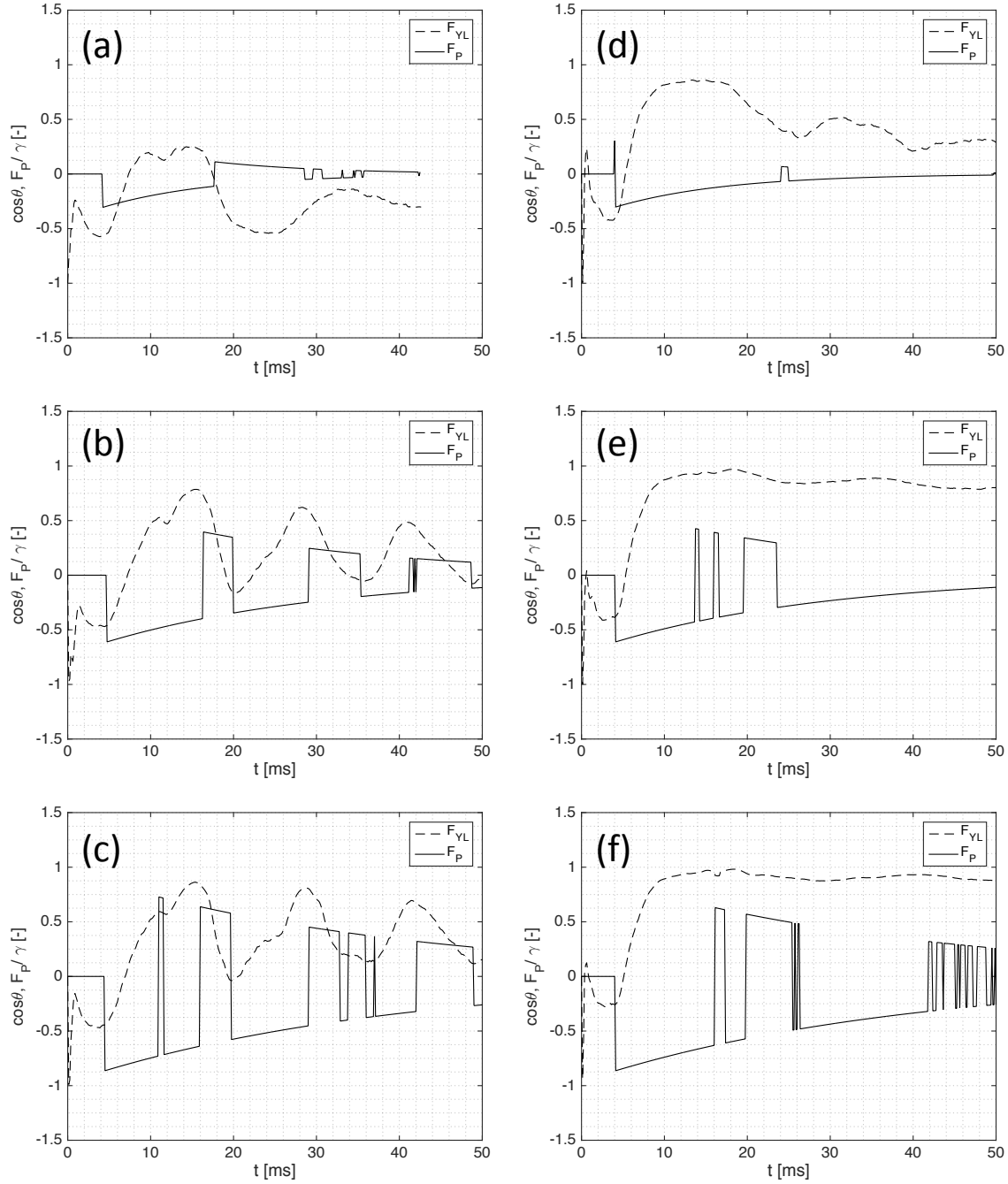

Figure 8. Dimensionless polymer force, F_P/γ, and dimensionless surface force $\cos\theta$, for impact Weber numbers We = 15 (a-c) and We = 80 (d-f), and polymer concentrations of 50 ppm (a,d), 200 ppm (b,e) and 400 ppm (c,f).

Conclusions

A modified Young-Laplace approach including a dissipative term representing the recall force of stretched polymer molecules at the contact line is proposed to explain the impact behaviour of dilute polymer solution drops as opposed to the behaviour of drops of pure solvent. Based on the ensemble of experimental observations in the past 20 years, it was concluded polymer stretching occurs as a supercritical coil-stretch transition in the shear flow generated during the inertial expansion of the drop on the target surface. Thus, the average polymer force can be modelled following the classical finite extensibility approach.

Preliminary results are in qualitative and quantitative agreement with experimental data from drop impact experiments, which however reveal the liquid inertia plays an important role in the drop impact dynamics.

Nomenclature

A	symmetric part of velocity gradient [s^{-1}]
c	mass concentration [-]

D	drop base diameter [m]
F	force [N]
h	liquid wedge thickness [m]
k_B	Boltzmann's constant [J/K]
L	polymer molecule length [m]
l	fractional extension of a polymer coil [-]
M	molecular mass [Da]
m	mass [kg]
N_A	Avogadro's number [mol^{-1}]
n	number density [-]
R	radius [m]
T	temperature [K]
t	time [s]
U	velocity [m/s]
V	contact line velocity [m/s]
Z	number of monomers [-]
η	viscosity [Pa $\cdot$ s]
γ	surface tension [N/m]
ρ	density [kg/m^3]
τ	relaxation time [s]
θ	apparent contact angle [$^\circ$]
ω	anti-symmetric part of velocity gradient [s^{-1}]
$\mathcal{L}^{-1}$	inverse Langevin function [-]

References

[1] Bergeron, V., Bonn, D., Martin, J.-Y., Vovelle, L., 2000, *Nature*, 405, pp. 772-775.
[2] Crooks, R., Cooper-White, J., Boger, D.V., 2001, *Chemical Engineering Science*, 56, pp. 5575-5592.
[3] Bartolo, D., Boudaoud, A., Narcy, G., Bonn, D., 2007, *Physical Review Letters*, 99 (17), 174502.
[4] Bertola, V., 2013, *Advances in Colloid and Interface Science*, 193-194, pp. 1-11.
[5] Rozhkov, A.N., Prunet-Foch, B., Vignes-Adler, M., 2002, *Physics of Fluids*, 15, pp. 2006-2019.
[6] Smith, M.I., Bertola, V., 2010, *Physical Review Letters*, 104 (15), 154502.
[7] Smith, M.I., Bertola, V., 2011, *Experiments in Fluids*, 50 (5), pp. 1385-1391.
[8] Bertola, V., 2010, *Colloids and Surfaces A: Physicochemical and Engineering Aspects*, 353 (1-3), pp. 135-140.
[9] Bertola, V., Wang, M., 2015, *Colloids and Surfaces A: Physicochemical and Engineering Aspects*, 481, pp. 600-608.
[10] Smith, M.I., Sharp, J.S., 2014, *Langmuir*, 30, pp. 5455-5459.
[11] Biolè, D., Bertola, V., Sep. 1.-4. 2013, 25th European Conference on Liquid Atomization and Spray Systems.
[12] Biolè, D., Bertola, V., 2015, *Archives of Mechanics*, 67 (5), pp. 401-414.
[13] Bertola, V., 2004, *Experiments in Fluids*, 37 (5), pp. 653-664.
[14] Smith, M.I., Bertola, V., Sep. 6.-8. 2010, 23rd European Conference on Liquid Atomization and Spray Systems.
[15] Biolè, D., Bertola, V., 2015, *Colloids and Surfaces A: Physicochemical and Engineering Aspects*, 467, pp. 149-156.
[16] Teraoka, I., 2002, "Polymer Solutions: An Introduction to Physical Properties". John Wiley & Sons.
[17] Brandrup, J., Immergut, E.H., Grulke, E.A., Abe, A., Bloch, D.R., 2005, "Polymer Handbook (4th Edition)". John Wiley & Sons.
[18] Kalashnikov, V.N., Askarov, A.N., 1989, *Journal of Engineering Physics*, 2, pp. 874-878.
[19] Glass, J.E., 1968, *Journal of Physical Chemistry*, 72, pp. 4459-4467.
[20] Lumley, J.L., 1973, *Journal of Polymer Science: Macromolecular Reviews*, 7 (1), pp. 263-290.
[21] de Gennes, P.G., 1974, *The Journal of Chemical Physics*, 60 (12), pp. 5030-5042.
[22] Peterlin, A., 1966, *Pure and Applied Chemistry*, 12 (1-4), pp. 563-586.
[23] Kroger, M., 2015, *Journal of Non-Newtonian Fluid Mechanics*, 223, pp. 77-87.
[24] Smith, D.E., Babcock, H.P., Chu, S., 1999, *Science*, 283, pp. 1724-1727.
[25] Bensimon, A., Simon, A., Chiffaudel. A., Croquette, V., Heslot, F., Bensimon, D., 1994, *Science*, 265, pp. 2096-2098.
[26] Tadmor, R., 2011, *Soft Matter*, 7, pp. 1577-1580.